

# Galectin-1 alleviates myocardial ischemia-reperfusion injury by reducing the inflammation and apoptosis of cardiomyocytes

DENGKE OU<sup>1</sup>, DAN NI<sup>2</sup>, RONG LI<sup>3</sup>, XIAOBO JIANG<sup>1</sup>, XIAOXIAO CHEN<sup>1</sup> and HONGFEI LI<sup>1</sup>

Departments of <sup>1</sup>Cardiovascular Medicine, <sup>2</sup>Nuclear Medicine and <sup>3</sup>Interventional Therapy, Chengdu Fifth People's Hospital, Chengdu, Sichuan 611130, P.R. China

Received June 7, 2020; Accepted September 16, 2021

DOI: 10.3892/etm.2021.11066

**Abstract.** Myocardial ischemia-reperfusion injury (MIRI) is one of the leading causes of morbidity and mortality worldwide, for which there is no effective treatment. The present study aimed to assess novel methods of clinical MIRI treatment by studying the effects of galectin-1 (Gal-1) on MIRI. Male 2-month-old Sprague Dawley rats and the rat cardiomyocyte cell line H9c2 were utilized in the present study. A rat model of MIRI was constructed by ligating the left anterior descending coronary artery, which was subsequently treated with Gal-1. Differences in myocardial injury were then assessed by hematoxylin and eosin (H&E) staining. In addition, the levels of inflammation and apoptosis in rat myocardial tissue were determined by immunohistochemistry staining. Hypoxia-reoxygenation was used to construct a model of MIRI in H9c2 cells. The effect of Gal-1 on the apoptosis and viability of H9c2 cells was also verified by flow cytometry and a Cell Counting Kit-8 assay. The results of H&E staining revealed that Gal-1 alleviated MIRI. Echocardiography demonstrated that Gal-1 improved cardiac function in rats following MIRI. In addition, MIRI increased levels of inflammation and apoptosis in rat myocardial tissues, with Gal-1 treatment reversing this effect. In cellular experiments, Gal-1 served anti-inflammatory and anti-apoptotic effects in hypoxic/reoxygenated cardiomyocytes. In conclusion, Gal-1 served a significant protective effect on the myocardial tissue after ischemia-reperfusion by reducing the level of inflammation and apoptosis in cardiomyocytes.

## Introduction

Ischemic heart disease is one of the leading causes of morbidity and mortality worldwide (1). Clinically, the most

effective intervention for myocardial ischemia is the restoration of blood flow perfusion, which reduces myocardial cell apoptosis, narrows the area of myocardial infarction and reverses cardiac dysfunction (2). However, reperfusion can also aggravate myocardial injury and myocardial cell death, in a process known as myocardial ischemia-reperfusion injury (MIRI) (3). Reperfusion itself can induce the excessive production of reactive oxygen species, excessive inflammatory response and cell apoptosis, aggravating myocardial injury and cell death (4). However, current available treatment strategies for MIRI are limited (5). Therefore, it is important to elucidate novel therapies to reduce MIRI in patients with ischemic heart disease, which can help to prevent and reverse the occurrence and development of MIRI, in turn improving their prognoses.

The underlying mechanism of MIRI remains poorly understood. At the time of MIRI, it is hypothesized that increases in oxygen free radicals, accumulation of neutrophils, slow blood flow or no reflow of occluded blood vessels caused by cellular swelling and myocardial cell calcium overload are all involved in the occurrence of myocardial injury (6). Changes in cells or tissues during MIRI can result in the increased production of oxygen free radicals, which in turn leads to breakage of peptide chains and destruction of the cellular membrane (7). Therefore, intracellular ATP production is reduced and cellular energy metabolism is significantly affected (7). In addition, destruction of cell membranes makes it easier for inflammatory cells to adhere to blood vessels, resulting in microcirculatory disorder and cell damage (8). Therefore, reducing oxidative stress and the inflammatory response during MIRI is key to effectively treating this disease.

The galectin (Gal) family represents a group of endogenous lectins with high affinities for polysaccharides containing  $\beta$ -galactoside residues (9). To date, 15 members of the lectin family have been identified, all of which contain highly conserved sugar recognition domains (9). Gal-1 is a member of the Gal family that is expressed in various types of cell, including thymic epithelial cells, endothelial cells, dendritic cells, macrophages, fibroblasts and bone marrow stromal cells (9-11). It is particularly abundant in skeletal muscle, smooth muscle, myocardium, sensory and motor neurons, and the placenta (10). Gal-1 has been reported to mediate a variety of biological functions that regulate the level of inflammation and apoptosis in cells. Huang *et al* (11) used lipopolysaccharide (LPS) to induce acute lung injury in mice, and found that

---

*Correspondence to:* Dr Hongfei Li, Department of Cardiovascular Medicine, Chengdu Fifth People's Hospital, 33 Mashu Street, Wenjiang, Chengdu, Sichuan 611130, P.R. China  
E-mail: honglan19690411@163.com

**Key words:** galectin-1, myocardial ischemia-reperfusion injury, inflammation, apoptosis

Gal-1 attenuated LPS-induced lung injury and reduced inflammation, oxidative stress and apoptosis. However, there is a lack of knowledge on the possible role of Gal-1 in MIRI. Therefore, the present study constructed a rat MIRI model and a model of MIRI in H9c2 cells. Gal-1 treatment was then applied to assess the effects of Gal-1 on MIRI.

## Materials and methods

**Animals and grouping.** A total of 60 2-month-old male Sprague-Dawley rats (weight, 250-350 g) were purchased from Charles River Laboratories, Inc. and housed in a temperature-controlled room ( $21\pm 2^\circ\text{C}$ ) on a 12-h light/dark cycle (lights on at 06:00) with a relative humidity range of 30-40%. Animal health and behavior was monitored daily. The present study was approved by the Animal Ethics Committee of Chengdu Fifth People's Hospital Animal Center (Chengdu, China). Rats were housed in a standard environment, receiving rat food and clean drinking water *ad libitum*. Rats were randomly divided into the following groups ( $n=15$  per group): i) Control; ii) Gal-1; iii) MIRI; and iv) MIRI + Gal-1. Animals in the Gal-1 and MIRI + Gal-1 groups were injected subcutaneously with Gal-1 ( $5\ \mu\text{g/g}$ ; Invitrogen; Thermo Fisher Scientific, Inc.) once per day, 1 week prior to modeling (12). Rats in the control group underwent the same anesthetic and surgical procedures but without ligation of the left anterior descending coronary artery.

**MIRI induction.** After anesthetizing rats with an intraperitoneal injection of pentobarbital sodium at a dose of 40 mg/kg, rats were placed on the operating table in the supine position. A small animal ventilator was used to maintain breathing. Surgical scissors were subsequently used to gently cut the left side of the chest to expose the heart. After locating the left anterior descending coronary artery, a suture was introduced to perform gentle ligation. After 30 min, the suture was untied for the recanalization of the left anterior descending coronary artery for 2 h (6). Echocardiography was subsequently performed to monitor animal cardiac function, which included the following parameters: Left ventricular end-systolic volume (ESV), left ventricular end-diastolic volume (EDV), left ventricular end-systolic diameter (LVIDs) and left ventricular end-diastolic diameter (LVIDd). Two rats in each of the MIRI and MIRI + GAL-1 groups died due to postoperative bleeding. At 2 h after reperfusion, the remaining 56 rats were euthanized via cervical dislocation after being anesthetized via intraperitoneal injection of pentobarbital sodium at a dose of 40 mg/kg, before heart and blood samples were collected. Cardiac arrest in the rats indicated that the rats were dead.

**Cell culture and treatment.** The rat cardiomyocyte H9c2 cell line (American Type Culture Collection) was cultured in DMEM (Gibco; Thermo Fisher Scientific, Inc.) supplemented with 10% FBS (Gibco; Thermo Fisher Scientific, Inc.), 1% streptomycin ( $100\ \mu\text{g/ml}$ ) and 1% penicillin ( $100\ \text{U/ml}$ ) at pH 7.4 in a 5%  $\text{CO}_2$  incubator at  $37^\circ\text{C}$ . Hypoxia-reoxygenation (HR) was used to construct an *in vitro* model of MIRI in H9c2 cells. To mimic myocardial I/R *in vitro*, H9c2 cells at 80% confluence were incubated in DMEM without FBS (previously bubbled with gas mixture containing 95%  $\text{N}_2$  and 5%  $\text{CO}_2$ ) for

6 h at  $37^\circ\text{C}$ . The cells were provided with fresh medium and then moved to 95%  $\text{O}_2/5\% \text{CO}_2$  for reoxygenation. The control plates were kept in the incubator with 95%  $\text{O}_2/5\% \text{CO}_2$  at  $37^\circ\text{C}$ . Cells were harvested 16 h post-reoxygenation for analysis.

**Ultrasonic cardiogram.** At 2 h following recanalization, rats were placed in the left lateral position and cardiac function was assessed using Philips ultrasound equipment (Philips iE33; Philips Medical Systems B.V.). Left ventricular ESV, left ventricular EDV, LVIDs and LVIDd were all measured. Left ventricular ejection fraction (EF) was calculated using the following formula:  $\text{EF}=(\text{EDV}-\text{ESV})/\text{EDV}$ . Additionally, fraction shortening (FS) was calculated the following formula:  $\text{FS}=(\text{LVIDd}-\text{LVIDs})/\text{LVIDd}$ .

**Hematoxylin and eosin staining.** Rat myocardial tissue was fixed with 4% paraformaldehyde at  $4^\circ\text{C}$ . After 24 h, myocardial tissue was dehydrated and embedded in paraffin. A microtome was subsequently used to section the myocardial tissue (thickness,  $5\ \mu\text{m}$ ). Sections were dewaxed, hydrated and stained with hematoxylin solution (Beyotime Institute of Biotechnology) for 1 min at  $37^\circ\text{C}$ . After rinsing sections for 3 min with running water, excess stain was removed with hydrochloric acid alcohol (Beyotime Institute of Biotechnology). Samples were then immersed in eosin solution (Beyotime Institute of Biotechnology) for 1 min and dehydrated at  $37^\circ\text{C}$ . Neutral gum was used to seal sections. Images were acquired using a light microscope (Nikon/80i; Nikon Corporation) and a digital camera (DP71CCD; Olympus Corporation).

**Immunohistochemical(IHC)staining.** After paraffin-embedded myocardial tissue was dewaxed and hydrated, sections ( $5\ \mu\text{m}$ ) were placed in citrate buffer and microwaved for 20 min. After the water was naturally cooled, sections were treated with 3% hydrogen peroxide for 30 min at  $37^\circ\text{C}$ . Subsequently, 10% goat serum (Beyotime Institute of Biotechnology) was used to treat sections for 1 h at  $37^\circ\text{C}$ . Samples were then incubated with the following primary antibodies at  $4^\circ\text{C}$  overnight (all Abcam, all 1:100): IL-1 $\beta$  (cat. no. ab9722), IL-6 (cat. no. ab6672), caspase-3 (cat. no. ab4051) and caspase-8 (cat. no. ab25901). Subsequently, sections were washed with PBS and incubated with secondary antibodies (Abcam). After DAB and hematoxylin staining, the slides were dehydrated, cleared with xylene, mounted with permanent mounting medium, then photographed via light microscopy (Nikon/80i; Nikon Corporation). The resulting images were analyzed by Image Pro-plus 6.0 software (Media Cybernetics, Inc.).

**RNA isolation and reverse transcription-quantitative PCR (RT-qPCR).** Total RNA was extracted from left ventricular anterior wall tissues of rats and H9c2 cells using TRIzol® (Invitrogen; Thermo Fisher Scientific, Inc.) according to the manufacturer's protocols. After determining the concentration of extracted RNA using a spectrophotometer, RNA was reverse transcribed into cDNA using an RT-qPCR kit (Invitrogen; Thermo Fisher Scientific, Inc.) according to the manufacturer's protocols. The SYBR Green Master Mix (Invitrogen; Thermo Fisher Scientific, Inc.) was used to amplify cDNA. The total reaction system volume was  $25\ \mu\text{l}$ . The thermocycling conditions were as follows: Pre-denaturation at  $95^\circ\text{C}$

Table I. Primer sequences.

Name	Forward/reverse	Sequence (5'-3')
IL-1 $\beta$	Forward	CCCTTGACTTGGGCTGT
	Reverse	CGAGATGCTGCTGTGAGA
IL-8	Forward	GAGCAACCCATACCCATCGA
	Reverse	TGGTCCCACCATATCTTCTTAATCT
TNF- $\alpha$	Forward	CAGCCAGGAGGGGAGAAC
	Reverse	GTATGAGAGGGACGGAACC
Caspase-3	Forward	GGAACGCGAAGAAAAGTG
	Reverse	ATTTTGAATCCACGGAGGT
Caspase-8	Forward	CACATCCCGCAGAAGAAG
	Reverse	GATCCCGCCGACTGATA
Bax	Forward	GAGGTCTTCTTCCGTGTGG
	Reverse	GATCAGCTCGGGCACTTT
Bcl-2	Forward	AGGAACTCTTCAGGGATGG
	Reverse	GCGATGTTGTCCACCAG
GAPDH	Forward	ATGGCTACAGCAACAGGGT
	Reverse	TTATGGGGTCTGGGATGG

for 5 min, followed by 35 cycles of denaturation at 95°C for 30 sec, annealing at 60°C for 45 sec, extension at 72°C for 3 min and a final extension at 72°C for 5 min. PCR products were stored at 4°C. The primers used for cDNA amplification were constructed by Genaray Biotech Co., Ltd. and are listed in Table I. Using the 2<sup>- $\Delta\Delta C_q$</sup>  method (13), the expression of endogenous GAPDH was used as the reference gene to calculate the expression of each mRNA.

**Immunofluorescence (IF) staining.** H9c2 cells were fixed using 4% paraformaldehyde at 4°C for 1 h and treated with PBS containing 0.2% Triton X-100 for 15 min at 4°C. After blocking with 10% goat serum at 4°C for 30 min, cells were incubated with primary antibodies against caspase-3 and caspase-8 (the same as the above) at 4°C overnight. After washing with PBS, cells were incubated with fluorescent secondary antibodies, including Alexa Fluor 546 goat anti-mouse IgG (H+L; 1:200; cat. no. A11030; Invitrogen; Thermo Fisher Scientific, Inc.) and donkey anti-rabbit-CY3 (1:200; cat. no. A21206; Molecular Probes; Thermo Fisher Scientific, Inc.) at 4°C for 2 h at room temperature. Samples were then stained with DAPI (Fluoroshield with DAPI; cat. no. F6057; Gibco; Thermo Fisher Scientific, Inc.) for 5 min at 4°C, washed with PBS and observed under a fluorescent microscope (Leica DM3000; Leica Microsystems GmbH; magnification, x60).

**ELISA.** Myocardial tissue of the left ventricular anterior wall of each rat was removed and lysed with RIPA (Beyotime Institute of Biotechnology). Rat blood samples were collected by cardiac puncture. Rat serum was then isolated by centrifugation (2,200 x g for 15 min, 4°C) and the resultant supernatant was stored at -80°C. ELISA kits (all Invitrogen; Thermo Fisher Scientific, Inc.) were subsequently used to determine the concentrations of creatine kinase (CK; cat. no. A032-1-1), lactate dehydrogenase (LDH; cat. no. A020-2-2), IL-6 (cat. no. H007-1-1), IL-8 (cat. no. H008) and TNF- $\alpha$

(cat. no. H052-1) (all, Nanjing Jiancheng Bioengineering Institute) in the lysate according to the manufacturer's protocols. Inflammatory factors in the supernatants of H9c2 cells were similar to that of myocardial tissue.

**Cell counting kit-8 (CCK-8) assay.** H9c2 cells were seeded into 96-well plates at a density of 3.0x10<sup>4</sup> cells/ml. After confluence reached 50%, various concentrations of Gal-1 (1, 3, 5, 10 and 20  $\mu$ M) were used to treat H9c2 cells (after hypoxia/reoxygenation). After 24 h at 20°C, 10  $\mu$ M CCK-8 reagent (Invitrogen; Thermo Fisher Scientific, Inc.) was added into each well of the 96-well plate. After a 2 h incubation at 20°C, a microplate reader (cat. no. HBS-1096A; Nanjing Detie Experimental Equipment Co., Ltd.) was used to measure the absorbance of each well at 450 nm.

**Flow cytometry.** Apoptosis rate was determined using flow cytometry. A cellular sieve (Beyotime Institute of Biotechnology) was utilized to extract cardiomyocytes from the rat myocardium, after which an Annexin V-FITC kit (Shanghai GeneChem Co., Ltd.) was used to detect the apoptotic rate of cardiomyocytes in accordance with the manufacturer's protocol. H9c2 cells were collected when the cell density reached 50%. The cells were then resuspended in 500  $\mu$ l Binding buffer. Annexin V (5  $\mu$ l) and PI (10  $\mu$ l) were added into Binding buffer, after which cells were incubated in the dark for 5 min at room temperature. Early apoptotic cells were presented in the lower right quadrant of the plot, while late apoptotic and necrotic cells were demonstrated in the upper right quadrant of the plot. A flow cytometer (FACSCalibur; BD Biosciences) was used for analysis. Data were obtained and analyzed using CellQuest professional software (Version 3.3; Becton-Dickinson and Company).

**Statistical analysis.** SPSS 20.0 (IBM Corp.) and GraphPad Prism 7.0 (GraphPad Software, Inc.) software were used for

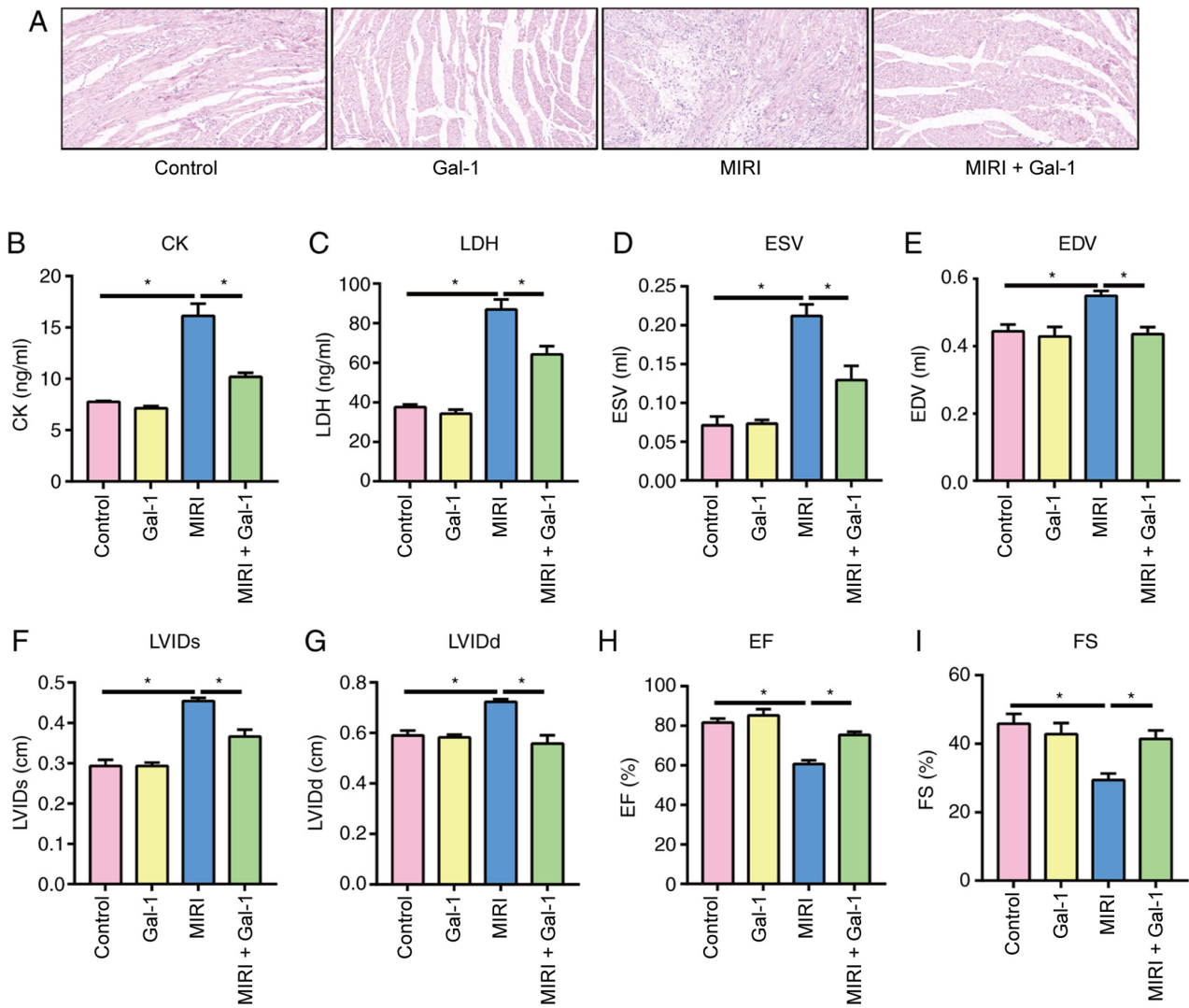


Figure 1. Galectin-1 attenuates myocardial ischemia-reperfusion injury and improves cardiac function in rats. (A) Representative H&E staining images of rat myocardial tissues. Magnification, x200. ELISA results of (B) CK and (C) LDH in rat serum. Results of rat echocardiography, including (D) ESV, (E) EDV, (F) LVIDs, (G) LVIDd, (H) EF and (I) FS. \* $P < 0.05$ . CK, creatine kinase; LDH, lactate dehydrogenase; MIRI, myocardial ischemia-reperfusion injury; ESV, left ventricular end-systolic volume; EDV, left ventricular end-diastolic volume; LVIDs, left ventricular end-systolic diameter; LVIDd, left ventricular end-diastolic diameter; EF, left ventricular ejection fraction; FS, fraction shortening; Gal-1, galectin-1.

statistical analysis. All experiments were repeated in triplicate and experimental data were expressed as the mean  $\pm$  standard deviation. Comparisons between multiple groups were performed using one-way ANOVA followed by Bonferroni post hoc test.  $P < 0.05$  was considered to indicate a statistically significant difference.

## Results

**Gal-1 treatment attenuates MIRI and improves cardiac function in rats.** To determine the potential effects of Gal-1 on rat myocardial tissue, H&E staining was performed to detect morphological changes after inducing MIRI. The results revealed that the structure of the myocardial tissue from rats in the MIRI group was disordered, and the number of cardiomyocytes was markedly decreased (Fig. 1A). By contrast, morphology of the tissues from rats in the MIRI + Gal-1 group was visibly improved compared with that in the MIRI group (Fig. 1A). There was no marked difference in the

morphology of myocardial tissues between the Gal-1 and the control groups. ELISA was subsequently performed to detect the levels of CK (Fig. 1B) and LDH (Fig. 1C) in rat serum. The results demonstrated that Gal-1 reduced the levels of CK and LDH at the MIRI level. Echocardiography was next performed to determine rat cardiac function (Fig. 1D-I). The ESV, EDV, LVIDs and LVIDd of MIRI rats were significantly higher compared with those in the control group, whereas the EF and FS were found to be lower when compared with those in the control group. Gal-1 treatment significantly reversed the effects of MIRI on each of the aforementioned parameters of rat cardiac function (Fig. 1D-I).

**Gal-1 reduces inflammation after MIRI.** The expression of IL-1 $\beta$  and IL-6 was next detected in rat myocardial tissue via IHC staining (Fig. 2A). The expression of IL-1 $\beta$  and IL-6 in the myocardial tissue of the MIRI group was markedly higher compared with that in the control group, whilst tissues in the MIRI + Gal-1 treatment exhibited decreased IL-1 $\beta$  and



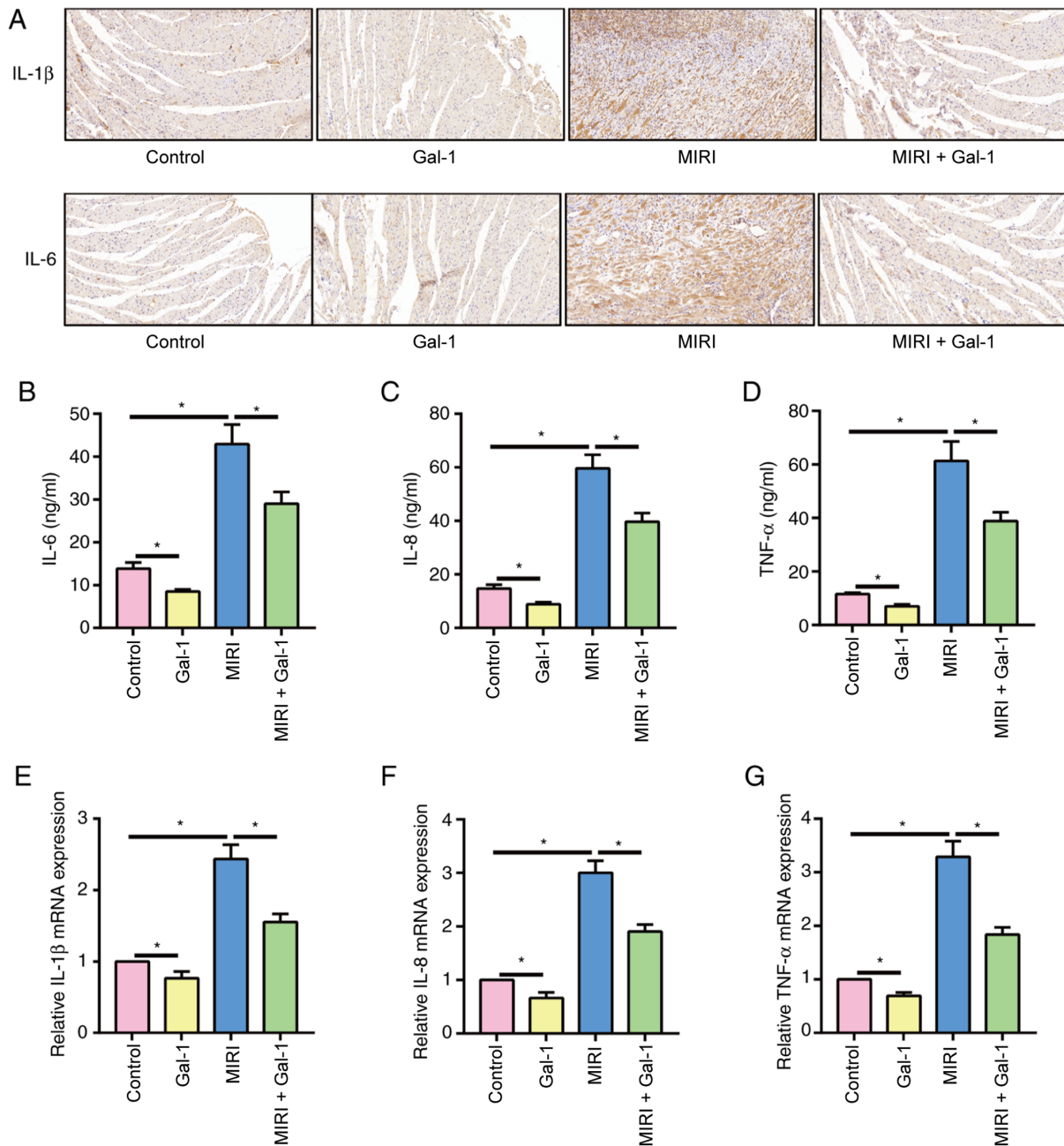


Figure 2. Galectin-1 reduces inflammation in rats after myocardial ischemia-reperfusion injury. (A) Representative immunohistochemistry staining images of IL-1 $\beta$  and IL-6 in rat myocardial tissues. Magnification, x200. ELISA results of (B) IL-6, (C) IL-8 and (D) TNF- $\alpha$ . mRNA expression levels of (E) IL-1 $\beta$ , (F) IL-8 and (G) TNF- $\alpha$  were measured. \*P<0.05. MIRI, myocardial ischemia-reperfusion injury; Gal-1, galectin-1.

IL-6 staining compared with that in the MIRI alone group. In addition, at basal level, the expression level of IL-1 $\beta$  and IL-6 in the myocardial tissue of the Gal-1 group was also lower compared with that in the control group. The levels of inflammatory factors (IL-6, IL-8 and TNF- $\alpha$ ) in rat serum were next measured by performing ELISA (Fig. 2B-D). The results revealed that Gal-1 significantly reduced their expression in rat serum. The results of RT-qPCR also confirmed the anti-inflammatory effect of Gal-1 on rat MIRI (Fig. 2E-G). In summary, IL-1 $\beta$ , IL-6, IL-8 and TNF- $\alpha$  increased after MIRI, but were reduced after treatment with Gal-1.

*Gal-1 reduces cardiomyocyte apoptosis after MIRI.* The expression of caspase-3 and -8 was assessed in rat myocardial tissue

following IHC staining. The results of IHC staining revealed that the expression of caspase-3 and -8 was markedly increased in myocardial tissue after MIRI, whilst Gal-1 treatment decreased the expression of caspase-3 and caspase-8 compared with that at basal and MIRI alone (Fig. 3A). The expression of caspase-3, caspase-8, Bax and Bcl-2 mRNA in rat myocardial tissue was next detected using RT-qPCR (Fig. 3B-E). Similar to the results of IHC staining, Gal-1 treatment also significantly reduced the expression of caspase-3, -8 and Bax and Bcl-2 mRNA. In addition, the apoptotic rate of rat cardiomyocytes was assessed via flow cytometry. The results demonstrated that rat cardiomyocyte apoptosis was significantly increased in the MIRI group compared with that in the control group, which was significantly reversed by Gal-1 treatment (Fig. 3F).

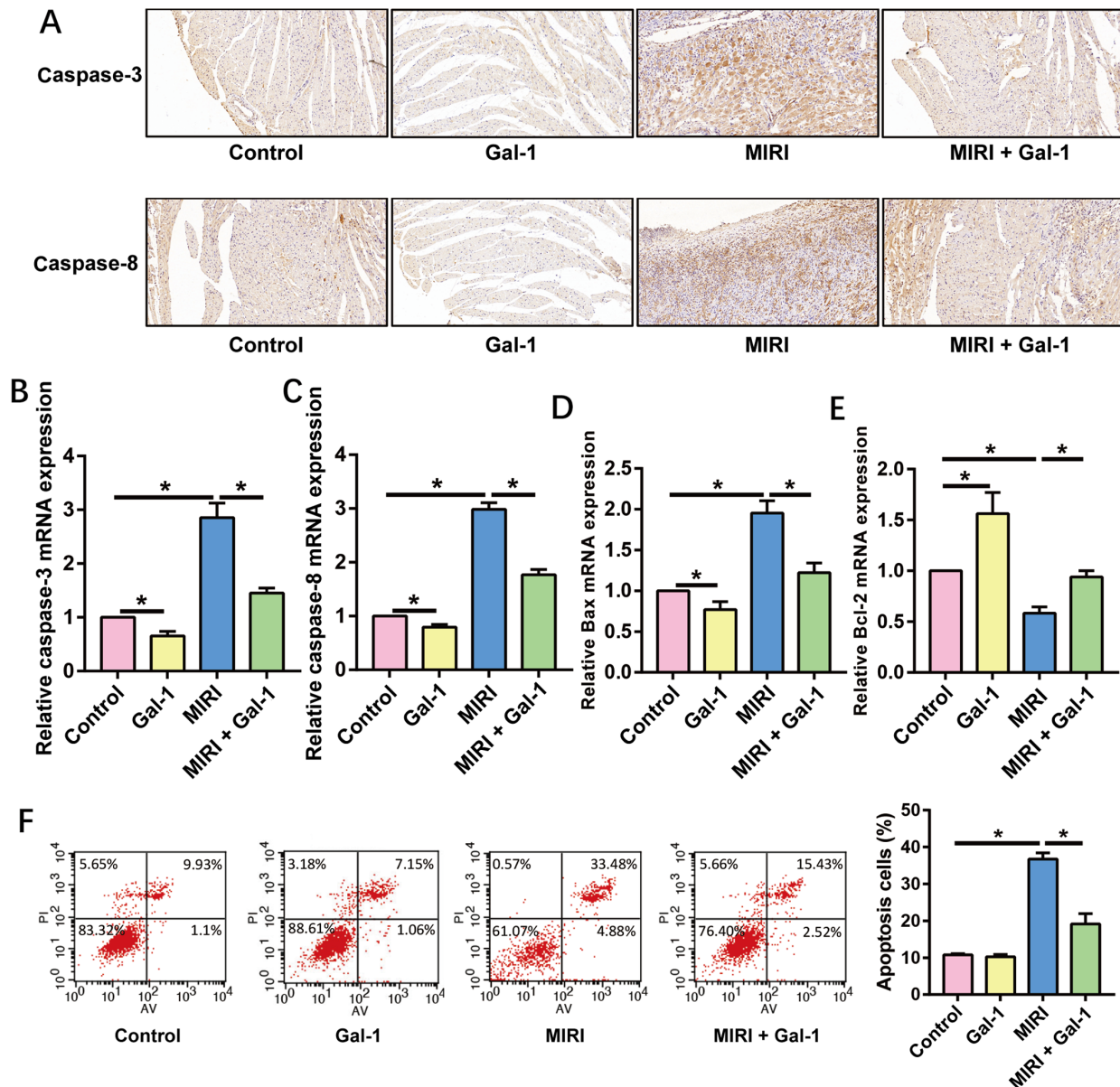


Figure 3. Galactin-1 reduces cardiomyocyte apoptosis after myocardial ischemia-reperfusion injury. (A) Representative immunohistochemistry staining images of caspase-3 and caspase-8 in rat myocardial tissues. Magnification,  $\times 200$ . mRNA expression levels of (B) caspase-3, (C) caspase-8, (D) Bax and (E) Bcl-2 was determined. (F) Apoptosis rate of cardiomyocytes was assessed.  $P < 0.05$ . MIRI, myocardial ischemia-reperfusion injury; Gal-1, galactin-1; AV, Annexin V.

*Gal-1 reduces inflammation and apoptosis in H9c2 cells.* To verify the potential effects of Gal-1 on cardiomyocytes, H9c2 cells were cultured, and the effects of Gal-1 on inflammation and apoptosis were determined. The effect of different concentrations of Gal-1 (1, 3, 5, 10 and 20  $\mu\text{M}$ ) on the viability of H9c2 cells was assessed by performing a CCK-8 assay. As the effect of 10  $\mu\text{M}$  Gal-1 on the viability of H9c2 cells under standard conditions was the most pronounced, this was used for subsequent experiments (Fig. 4A). The levels of IL-6 (Fig. 4B) and IL-8 (Fig. 4C) in H9c2 cell supernatants were also examined by ELISA. Gal-1 stimulation was determined to inhibit the inflammatory response of H9c2 cells induced by HR. Furthermore, IF staining revealed that the expression of caspase-3 and caspase-8 was decreased in H9c2 cells following Gal-1 stimulation (Fig. 4D and E). Gal-1 was also found to reduce the rate of apoptosis in H9c2 cells (Fig. 4F). Therefore, it was concluded that Gal-1 exerted anti-inflammatory and anti-apoptotic effects on H9c2 cells.

## Discussion

Ischemic heart disease is the main cause of death worldwide, accounting for  $>9$  million deaths in 2016 according to the World Health Organization estimates (4). In addition to drug treatment, reperfusion therapy can improve the symptoms and prognosis of patients with ischemic heart disease, in turn increasing the cure rate of acute myocardial infarction (4). However, irreversible damage to the myocardium may occur prior to treatment, leading to myocardial necrosis, electrical remodeling and anatomical remodeling of the ventricle (14). MIRI serves an important role throughout this process (15). Previous studies have shown that MIRI may be associated with cardiomyocyte apoptosis, excessive oxygen free radical production, calcium overload and inflammation (6,7,14). Gal-1 is closely associated with cardiac function and metabolism, which has been previously demonstrated to mediate cardiovascular

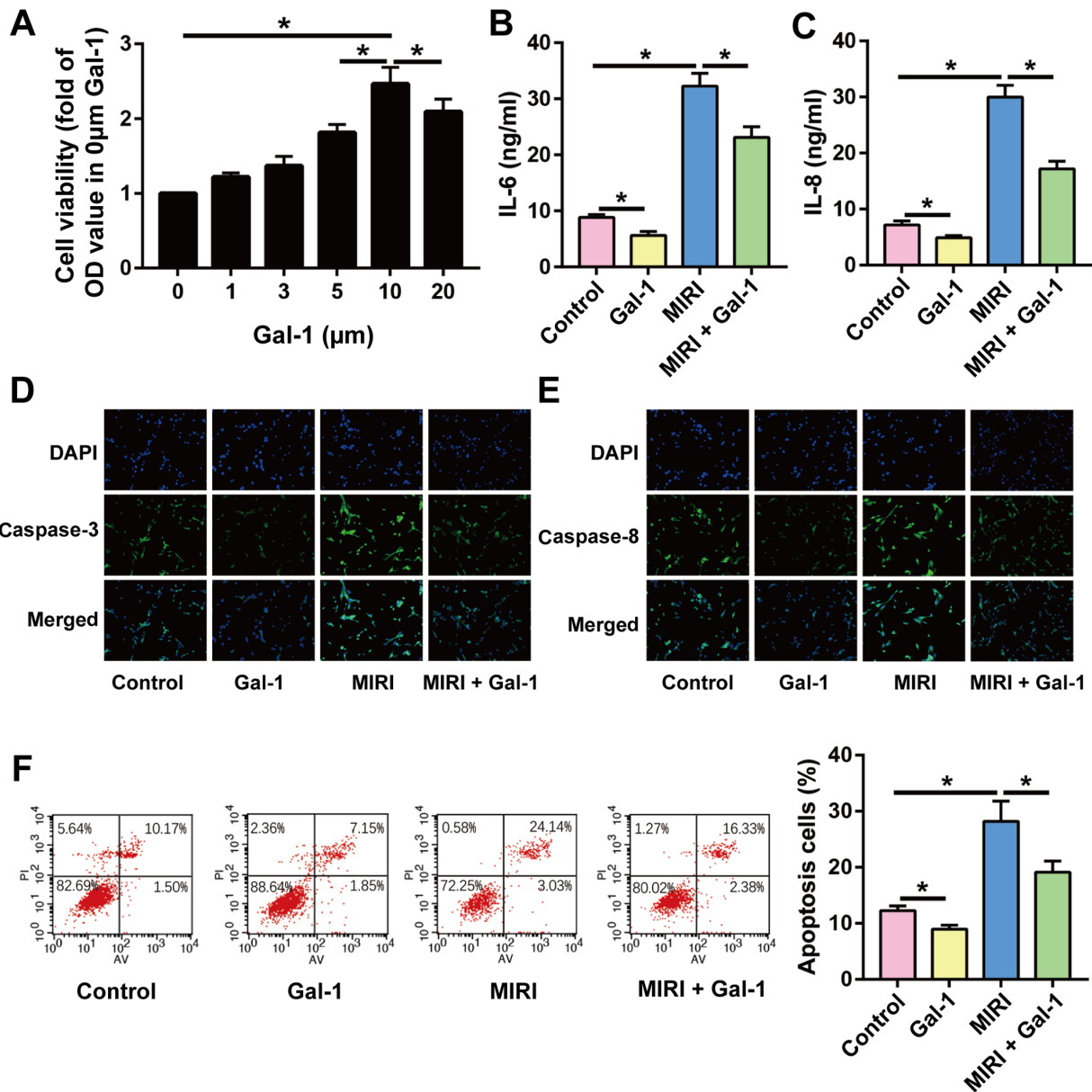


Figure 4. Galectin-1 reduces inflammation and apoptosis in H9c2 cells. (A) Cell Counting Kit-8 cell viability results for H9c2 cells are presented. ELISA was performed in the cell culture supernatants to detect (B) IL-6 and (C) IL-8 levels. Representative immunofluorescence staining images of (D) caspase-3 and (E) caspase-8 in H9c2 cells are presented. Magnification, x200. (F) Rate of apoptosis was calculated in H9c2 cells. \*P<0.05. MIRI, myocardial ischemia-reperfusion injury; Gal-1, galectin-1; AV, Annexin V.

inflammation, serving as an important therapeutic target for cardiovascular related diseases (15). A previous study revealed that Gal-1 alleviated myocardial hypertrophy by regulating calcium channels in 293 cells (16). In addition, Gal-1 inhibited myocardial inflammation and thus served a protective role in ventricular remodeling in a mouse model of acute myocardial infarction (17). The present study investigated the effects of Gal-1 on heart function, inflammation and apoptosis in the rat myocardium after MIRI. The results indicated that Gal-1 treatment improved MIRI-induced myocardial injury, and reduced the extent of inflammation and apoptosis in myocardial tissue. In addition, the protective effects of Gal-1 on cardiomyocytes were verified in H9c2 cells. These results may prove to be helpful for the clinical treatment of MIRI.

The inflammatory response is an important mechanism of MIRI, where a number of studies have confirmed that

anti-inflammatory therapy is beneficial to MIRI (15,18). MIRI promotes the production of various inflammatory cytokines, including IL-1, IL-6 and TNF- $\alpha$ , and promotes the infiltration of inflammatory cells to the myocardial tissue (15). A continuous inflammatory response not only affects the ischemic organ itself, but can also cause damage to other organs or tissues, potentially leading to multiple organ failure (19). In the present study, after rats were treated with Gal-1, the expression of inflammatory factors in the myocardial tissue and serum was significantly decreased. This suggested that Gal-1 is an important factor that improves heart function in rats. Related studies have also previously demonstrated that ischemia-reperfusion not only causes severe tissue injury, but also excessive inflammatory reactions by activating both innate and adaptive immune responses (6,7). Activation of the innate or adaptive immune response causes a large number of

inflammatory cells to be produced and activated, leading to inflammatory reactions in several organs.

Studies have previously demonstrated that leukocytes are involved in the process of ischemia-reperfusion injury (6,15). The earliest example of leukocyte involvement in ischemia-reperfusion injury was reported by Romson *et al* (20). Their results revealed that the administration of leukocytes with anti-leukocyte serum reduced the extent of myocardial infarction in dogs to the same extent as that mediated by oxygen radical scavengers, suggesting that leukocytes were involved in ischemia-reperfusion injury. Furthermore, Frey *et al* (21) revealed that after 3 h of myocardial ischemia in dogs, a large number of leukocytes accumulated in the capillaries, resulting in increased local vascular resistance, no reflow and tissue edema. In the same study, they also found that following anti-leukocyte administration, the number of capillaries without reflow was significantly reduced. In addition, capillary blockage was significantly reduced and the incidence of ventricular arrhythmia was also significantly reduced after treatment with caspase inhibitors in a rabbit cardiomyocyte ischemia reperfusion model (22). Although cell membrane damage occurs during ischemia-reperfusion, cell membrane-related degradation products increase (23). Certain degradation products, such as reactive oxygen species, have been reported to strongly mediate inflammatory chemotaxis, which results in a large number of leukocytes adsorbing to the vascular endothelium, increasing the number of leukocytes in the microcirculation and circulation surrounding the organ (24). During the process of ischemia-reperfusion, the release of a variety of intercellular adhesion molecules, such as intercellular cell adhesion molecule-1 and E-selectin, may cause neutrophil infiltration (25). The infiltration of neutrophils also embolizes part of the capillary blood vessel (25). After restoring blood perfusion, some ischemic tissues remain unable to achieve blood perfusion, which is the main reason for the occurrence of no-reflow after tissue ischemia-reperfusion (26). Therefore, the anti-inflammatory effects of Gal-1 on cardiomyocytes were largely proposed to ameliorate MIRI in the current study.

Apoptosis, also known as programmed cell death, is a form of active gene-regulated cell death (27). Cardiomyocyte apoptosis is an important factor mediating myocardial injury, determining the area of myocardial infarction and promoting myocardial remodeling (28,29). The apoptosis of cardiomyocytes may result in decreased systolic function, thereby leading to a decrease in cardiac pump function (30). In the present study, Gal-1 reduced the expression of the caspase family of proteins in cardiomyocytes and increased the ratio of Bcl-2 and Bax. The results of flow cytometry also demonstrated that Gal-1 reduced the rate of apoptosis in rat cardiomyocytes, indicating that cardiomyocyte apoptosis was suppressed during MIRI by Gal-1. Apoptosis is an important factor in MIRI (31). Apoptotic cells have been previously identified in rabbit models of MIRI, which further confirmed that apoptosis occurs in the marginal zone of myocardial infarction (32). Other studies using MIRI rabbit models confirmed that apoptosis did not occur after reperfusion for 4 h following myocardial ischemia for 5 min (33,34). Additionally, no myocardial apoptosis was detected after 30 min of ischemia (35). However, after ischemia for 30 min

and reperfusion for 4 h, cardiomyocytes exhibited marked apoptosis, suggesting that cardiomyocyte apoptosis is not only dependent on reperfusion injury, but also on the length of ischemia. A previous study utilizing dogs to establish an MIRI model revealed no obvious apoptosis after 7 h myocardial ischemia (36). Apoptosis was observed following ischemia for 1 h and reperfusion for 6 h. It is considered that apoptosis is more likely to occur in myocardial reperfusion (24). In a clinical study, myocardial tests were conducted in 8 patients who were diagnosed with acute myocardial infarction (37). Hemorrhagic infarction, spontaneous subintimal myocardial ischemia and reperfusion injury, and apoptosis around the infarction area were all found, indicating an association between MIRI and apoptosis (38). Therefore, apoptosis is an important mechanism of MIRI. Additionally, the anti-apoptotic effect of Gal-1 was hypothesized to improve myocardial cell survival and MIRI in the present study.

The activation of inflammatory cells and the release of inflammatory factors are important for cardiomyocyte apoptosis during MIRI (39). NF- $\kappa$ B is a key protein that regulates the immune response and proinflammatory cytokine expression (39). The NF- $\kappa$ B signal transduction pathway is closely associated with the production and release of pro-inflammatory cytokines and the occurrence of cardiomyocyte apoptosis (40). Previous studies reported that MIRI induces the activation of NF- $\kappa$ B, the inflammatory cascade of which promotes the occurrence of cardiomyocyte apoptosis (41,42). In addition, TNF- $\alpha$  has also been documented to increase vascular permeability, enhance neutrophil adhesion and induce cardiomyocyte apoptosis (43). IL-6 is a fast-acting inflammatory cytokine that responds to stress within the heart (44). IL-6 acts directly on cardiomyocytes to induce myocardial inhibition by altering the function of the sarcoplasmic reticulum and reducing the concentration of calcium ions in the cell cytoplasm (44). IL-6 has also been previously revealed to serve an important regulatory role in myocardial apoptosis in a rat model of MIRI (35). Therefore, the anti-inflammatory and anti-apoptotic effects of Gal-1 significantly alleviated MIRI in rats in the current study.

However, there were some limitations in the present study. MIRI is the result of multiple pathological mechanisms. The present study only investigated the effect of Gal-1 on inflammation and apoptosis during MIRI, but did not investigate the effect of Gal-1 on other pathological mechanisms of MIRI, such as oxidative stress and calcium ion overload. In addition, the target of Gal-1 in cardiomyocytes remains unclear. Therefore, the role of Gal-1 in MIRI requires further study; specifically, the target of Gal-1 needs to be identified through techniques such as gene sequencing.

In the present study, Gal-1 significantly alleviated the disorder of cardiomyocytes caused by MIRI and improved cardiac function in rats. In addition, MIRI was accompanied by an excessive inflammatory response with increased apoptosis in rat myocardial tissues, both of which were alleviated by Gal-1 treatment.

#### Acknowledgements

Not applicable.



## Funding

The current study was funded by the Chengdu Technical Innovation and Research Project: Mechanism and myocardial mechanical characteristics of rupture QRS in patients with hypertrophic cardiomyopathy: CMR multi-mode imaging study (grant no. 2019-YF05-00111-SN) and the Chengdu High-level Key Clinical Specialty Construction Project (grant no. 2021-5#).

## Availability of data and materials

The datasets used and/or analyzed during the current study are available from the corresponding author on reasonable request.

## Authors' contributions

DO and HL designed the study and performed the experiments, DO, DN and RL established the animal models, DO and XJ acquired the data, and HL and XC analyzed the data. All authors read and approved the final manuscript. DO and HL confirm the authenticity of all the raw data.

## Ethics approval and consent to participate

The present study was approved by the Animal Ethics Committee of Chengdu Fifth People's Hospital Animal Center (Chengdu, China).

## Patient consent for publication

Not applicable.

## Competing interests

The authors declare that they have no competing interests.

## References

- Popescu CP, Florescu SA, Hasbun R, Harxhi A, Evendar R, Kahraman H, Neuberger A, Codreanu D, Zaharia MF, Tosun S, *et al*: Prediction of unfavorable outcomes in West Nile virus neuroinvasive infection-Result of a multinational ID-IRI study. *J Clin Virol* 122: 104213, 2019.
- Henry JJD, Delrosario L, Fang J, Wong SY, Fang Q, Sievers R, Kotha S, Wang A, Farmer D, Janaswamy P, *et al*: Development of injectable amniotic membrane matrix for postmyocardial infarction tissue repair. *Adv Healthc Mater* 9: e1900544, 2020.
- Murthy SB, Diaz I, Wu X, Merkler AE, Iadecola C, Safford MM, Sheth KN, Navi BB and Kamel H: Risk of arterial ischemic events after intracerebral hemorrhage. *Stroke* 51: 137-142, 2020.
- GBD 2017 Disease and Injury Incidence and Prevalence Collaborators: Global, regional, and national incidence, prevalence, and years lived with disability for 354 diseases and injuries for 195 countries and territories, 1990-2017: A systematic analysis for the global burden of disease study 2017. *Lancet* 392: 1789-1858, 2018.
- Jackson CA, Kerssens J, Fleetwood K, Smith DJ, Mercer SW and Wild SH: Incidence of ischaemic heart disease and stroke among people with psychiatric disorders: Retrospective cohort study. *Br J Psychiatry* 217: 442-449, 2020.
- Gul-Kahraman K, Yilmaz-Bozoglan M and Sahna E: Physiological and pharmacological effects of melatonin on remote ischemic preconditioning after myocardial ischemia-reperfusion injury in rats: Role of Cybb, Fas, NfκB, irisin signaling pathway. *J Pineal Res* 67: e12589, 2019.
- Merz SF, Korste S, Bornemann L, Michel L, Stock P, Squire A, Soun C, Engel DR, Detzer J, Lörchner H, *et al*: Contemporaneous 3D characterization of acute and chronic myocardial I/R injury and response. *Nat Commun* 10: 2312, 2019.
- Stiermaier T, Jensen JO, Rommel KP, de Waha-Thiele S, Fuernau G, Desch S, Thiele H and Eitel I: Combined intrahospital remote ischemic preconditioning and postconditioning improves clinical outcome in ST-elevation myocardial infarction. *Circ Res* 124: 1482-1491, 2019.
- Tsai YT, Liang CH, Yu JH, Huang KC, Tung CH, Wu JE, Wu YY, Chang CH, Hong TM and Chen YL: A DNA aptamer targeting galectin-1 as a novel immunotherapeutic strategy for lung cancer. *Mol Ther Nucleic Acids* 18: 991-998, 2019.
- Kuroi K, Kamijo M, Ueki M, Niwa Y, Hiramatsu H and Nakabayashi T: Time-resolved FTIR study on the structural switching of human galectin-1 by light-induced disulfide bond formation. *Phys Chem Chem Phys* 22: 1137-1144, 2019.
- Huang XT, Liu W, Zhou Y, Sun M, Yang HH, Zhang CY and Tang SY: Galectin-1 ameliorates lipopolysaccharide-induced acute lung injury via AMPK-Nrf2 pathway in mice. *Free Radic Biol Med* 146: 2222-2233, 2020.
- Carlos CP, Silva AA, Gil CD and Oliani SM: Pharmacological treatment with galectin-1 protects against renal ischaemia-reperfusion injury. *Sci Rep* 8: 9568, 2018.
- Livak KJ and Schmittgen TD: Analysis of relative gene expression data using real-time quantitative PCR and the 2(-Delta Delta C(T)) method. *Methods* 25: 402-408, 2001.
- Lameijer H, Schutte JM, Schuitemaker NW, van Roosmalen JJ, Pieper PG, Dutch Maternal Mortality and Morbidity Committee: Maternal mortality due to cardiovascular disease in the Netherlands: A 21-year experience. *Neth Heart J* 28: 27-36, 2020.
- Seropian IM, González GE, Maller SM, Berrocal DH, Abbate A and Rabinovich GA: Galectin-1 as an emerging mediator of cardiovascular inflammation: Mechanisms and therapeutic opportunities. *Mediators Inflamm* 2018: 8696543, 2018.
- Fan J, Fan W, Lei J, Zhou Y, Xu H, Kapoor I, Zhu G and Wang J: Galectin-1 attenuates cardiomyocyte hypertrophy through splice-variant specific modulation of Ca<sub>v</sub>1.2 calcium channel. *Biochim Biophys Acta* 1865: 218-229, 2019.
- Seropian IM, Cerliani JP, Toldo S, Van Tassell BW, Ilarregui JM, González GE, Matoso M, Salloum FN, Melchior R, Gelpi RJ, *et al*: Galectin-1 controls cardiac inflammation and ventricular remodeling during acute myocardial infarction. *Am J Pathol* 182: 29-40, 2013.
- Han B, Li S, Lv Y, Yang D, Li J, Yang Q, Wu P, Lv Z and Zhang Z: Dietary melatonin attenuates chromium-induced lung injury via activating the Sirt1/Pgc-1α/Nrf2 pathway. *Food Funct* 10: 5555-5565, 2019.
- Yang Q, Han B, Xue J, Lv Y, Li S, Liu Y, Wu P, Wang X and Zhang Z: Hexavalent chromium induces mitochondrial dynamics disorder in rat liver by inhibiting AMPK/PGC-1α signaling pathway. *Environ Pollut* 265: 114855, 2020.
- Romson JL, Hook BG, Kunkel SL, Abrams GD, Schork MA and Lucchesi BR: Reduction of the extent of ischemic myocardial injury by neutrophil depletion in the dog. *Circulation* 67: 1016-1023, 1983.
- Frey UH, Klaassen M, Ochsenfarth C, Murke F, Thielmann M, Kottenberg E, Kleinbongard P, Klenke S, Engler A, Heusch G, *et al*: Remote ischaemic preconditioning increases serum extracellular vesicle concentrations with altered micro-RNA signature in CABG patients. *Acta Anaesthesiol Scand* 63: 483-492, 2019.
- Li HL, Karwatowska-Prokopeczuk E, Mutomba M, Wu J, Karanewsky D, Valentino K, Engler RL and Gottlieb RA: Pharmacology of caspase inhibitors in rabbit cardiomyocytes subjected to metabolic inhibition and recovery. *Antioxid Redox Signal* 3: 113-123, 2001.
- Abassi Z, Armaly Z and Heyman SN: Glycocalyx degradation in ischemia-reperfusion injury. *Am J Pathol* 190: 752-767, 2020.
- Gottlieb RA and Engler RL: Apoptosis in myocardial ischemia-reperfusion. *Ann N Y Acad Sci* 874: 412-426, 1999.
- Amar DN, Epshtein M and Korin N: Endothelial cell activation in an embolic ischemia-reperfusion injury microfluidic model. *Micromachines (Basel)* 10: 857, 2019.
- Gonzalez AL, Ciocci PA, Fantinelli JC, Rojano B, Schinella GR and Mosca SM: Isoespintanol, a monoterpene isolated from oxandra cf xylopioides, ameliorates the myocardial ischemia-reperfusion injury by AKT/PKCε/eNOS-dependent pathways. *Naunyn Schmiedebergs Arch Pharmacol* 393: 629-638, 2020.

27. Elmore S: Apoptosis: A review of programmed cell death. *Toxicol Pathol* 35: 495-516, 2007.
28. Li S, Baiyun R, Lv Z, Li J, Han D, Zhao W, Yu L, Deng N, Liu Z and Zhang Z: Exploring the kidney hazard of exposure to mercuric chloride in mice: Disorder of mitochondrial dynamics induces oxidative stress and results in apoptosis. *Chemosphere* 234: 822-829, 2019.
29. Liu B, Yu H, Baiyun R, Lu J, Li S, Bing Q, Zhang X and Zhang Z: Protective effects of dietary luteolin against mercuric chloride-induced lung injury in mice: Involvement of AKT/Nrf2 and NF- $\kappa$ B pathways. *Food Chem Toxicol* 113: 296-302, 2018.
30. Baiyun R, Li S, Liu B, Lu J, Lv Y, Xu J, Wu J, Li J, Lv Z and Zhang Z: Luteolin-mediated PI3K/AKT/Nrf2 signaling pathway ameliorates inorganic mercury-induced cardiac injury. *Ecotoxicol Environ Saf* 161: 655-661, 2018.
31. Zhu J, Wang YF, Chai XM, Qian K, Zhang LW, Peng P, Chen PM, Cao JF, Qin ZH, Sheng R and Xie H: Exogenous NADPH ameliorates myocardial ischemia-reperfusion injury in rats through activating AMPK/mTOR pathway. *Acta Pharmacol Sin* 41: 535-545, 2019.
32. Xu XZ, Luo B, Xiao Y and Zheng WQ: Effects of lncRNA MALAT1-mediated beta-catenin signaling pathway on myocardial cell apoptosis in rats with myocardial ischemia/reperfusion injury. *Eur Rev Med Pharmacol Sci* 23: 9557-9565, 2019.
33. Lazou A, Iliodromitis EK, Cieslak D, Voskarides K, Mousikos S, Bofilis E and Kremastinos DT: Ischemic but not mechanical preconditioning attenuates ischemia/reperfusion induced myocardial apoptosis in anaesthetized rabbits: The role of Bcl-2 family proteins and ERK1/2. *Apoptosis* 11: 2195-2204, 2006.
34. Wang N, Minatoguchi S, Chen X, Uno Y, Arai M, Lu C, Takemura G, Fujiwara T and Fujiwara H: Antidiabetic drug miglitol inhibits myocardial apoptosis involving decreased hydroxyl radical production and Bax expression in an ischaemia/reperfusion rabbit heart. *Br J Pharmacol* 142: 983-990, 2004.
35. Zhou BZ, Zhang DH, Yu WM and Ning JZ: Protective effect of cyclosporine A in the treatment of severe hydronephrosis in a rabbit renal pelvic perfusion model. *Turk J Med Sci* 49: 1590-1598, 2019.
36. Sheng X, Chen M, Huang B, Liu J, Zhou L, Bao M and Li S: Cardioprotective effects of low-level carotid baroreceptor stimulation against myocardial ischemia-reperfusion injury in canine model. *J Interv Card Electrophysiol* 45: 131-140, 2016.
37. Ho MY, Wen MS, Yeh JK, Hsieh IC, Chen CC, Hsieh MJ, Tsai ML, Yang CH, Wu VC, Hung KC, *et al*: Excessive irisin increases oxidative stress and apoptosis in murine heart. *Biochem Biophys Res Commun* 503: 2493-2498, 2018.
38. Abhari BA, McCarthy N, Agostinis P and Fulda S: NF- $\kappa$ B contributes to Smac mimetic-conferred protection from tunicamycin-induced apoptosis. *Apoptosis* 24: 269-277, 2019.
39. Toldo S, Mauro AG, Cutter Z and Abbate A: Inflammasome, pyroptosis, and cytokines in myocardial ischemia-reperfusion injury. *Am J Physiol Heart Circ Physiol* 315: H1553-H1568, 2018.
40. Nichols TC: NF-kappaB and reperfusion injury. *Drug News Perspect* 17: 99-104, 2004.
41. Qian Q, Cao X, Wang B, Qu Y, Qian Q, Sun Z and Feng F: TNF- $\alpha$ -TNFR signal pathway inhibits autophagy and promotes apoptosis of alveolar macrophages in coal worker's pneumoconiosis. *J Cell Physiol* 234: 5953-5963, 2019.
42. Chen H, Zhang RQ, Wei XG, Ren XM and Gao XQ: Mechanism of TLR-4/NF- $\kappa$ B pathway in myocardial ischemia reperfusion injury of mouse. *Asian Pac J Trop Med* 9: 503-507, 2016.
43. Groot HE, Ali LA, van der Horst IC, Schurer RA, van der Werf HW, Lipsic E, van Veldhuisen DJ, Karper JC and van der Harst P: Plasma interleukin 6 levels are associated with cardiac function after ST-elevation myocardial infarction. *Clin Res Cardiol* 108: 612-621, 2019.
44. Moreira DM, da Silva RL, Vieira JL, Fattah T, Lueneberg ME and Gottschall CA: Role of vascular inflammation in coronary artery disease: Potential of anti-inflammatory drugs in the prevention of atherothrombosis. Inflammation and anti-inflammatory drugs in coronary artery disease. *Am J Cardiovasc Drugs* 15: 1-11, 2015.



This work is licensed under a Creative Commons Attribution-NonCommercial-NoDerivatives 4.0 International (CC BY-NC-ND 4.0) License.